

Investigation of PET/MRI Image Fusion Schemes for Enhanced Breast Cancer Diagnosis

Karl G. Baum, *Member, IEEE*, Evan Schmidt, Kimberly Rafferty, Maria Helguera, *Member, IEEE*, David H. Feiglin, and Andrzej Krol, *Senior Member, IEEE*

Abstract—The benefit of registration and fusion of functional images with anatomical images is well appreciated in the advent of PET/CT. There is an increasing interest in expanding this approach to PET/MRI. The focus of much of the related research has been on registering images from different modalities. However, the importance of appropriately jointly displaying (i.e. fusing) the registered images has often been neglected and underestimated. Our aim is to determine which fusion techniques are most useful for enhanced diagnostic performance, ease of use, efficiency, and accuracy for reading registered MRI and PET breast images. Preliminary results indicate that the radiologists were better able to perform a series of tasks when reading the fused PET/MRI data sets using color tables generated by our new genetic algorithm, as compared to commonly used fire/gray or red/gray schemes.

I. INTRODUCTION

Application of a multimodality approach is advantageous for detection, diagnosis, and management of many ailments. Obtaining the spatial relationships between the modalities and conveying them to the observer maximizes the benefit that can be achieved.

The process of obtaining the spatial relationships and manipulating the images so that corresponding pixels in them represent the same physical location is called image registration. Combining the registered images into a single image is called image fusion.

The advantage of a fused image lies in our inability to accurately visually judge spatial relationships between images when they are viewed side by side. Depending on background texture, mottle, shades and colors, identical shapes and lines may appear to be different sizes [1]. This can be demonstrated by well-known simple optical illusions. The most obvious application is to combine a functional image that identifies a region of interest, but lacks structural information necessary for localization, with an anatomical image providing this information.

In this paper we examine the benefits of a multimodality approach in the context of breast cancer imaging. We then

briefly discuss a recently developed registration technique before launching into possible fusion options. An overview of fusion techniques widely accepted in literature, as well as a novel genetic algorithm-based one are briefly presented. The remainder of the text is devoted to a study in which radiologists were asked to perform a set of tasks reading fused PET/MRI breast images obtained using several different fusion techniques.

A. Multimodal Breast Cancer Imaging

Application of a multimodality approach is advantageous for detection, diagnosis and management of breast cancer. In this context, F-18-FDG positron emission tomography (PET) [2, 3], and high-resolution and dynamic contrast-enhanced magnetic resonance imaging (MRI) [4, 5] have steadily gained acceptance in addition to x-ray mammography and ultrasonography. Initial experience with combined PET (functional imaging) and x-ray computed tomography (CT, anatomical localization) has demonstrated sizable improvements in diagnostic accuracy, allowing better differentiation between normal (e.g. bowel) and pathological uptake and by providing positive finding in CT images for lesions with low metabolic activity [3].

A method was developed for the coregistration of PET and MRI images, to provide additional information on morphology (including borders, edema, and vascularization) and on dynamic behavior (including fast wash-in, positive enhancement intensity, and fast wash-out) of the suspicious lesion and to allow more accurate lesion localization including mapping of hyper- and hypo-metabolic regions as well as better lesion-boundary definition. Such information might be of great value for grading the breast cancer and assessing the need for biopsy. If biopsy is needed, it could be precisely guided to the most metabolically active (i.e. most malignant) region.

II. REGISTRATION

Since the breast is entirely composed of soft tissue, it easily deforms and requires nonrigid registration. Physically-based deformable breast models are very difficult to implement because of complex patient-specific breast morphology and highly nonlinear and difficult to measure elastic properties of different types of tissues in the breast, as well as explicitly unknown boundary conditions [6]. The approach presented

Manuscript received May 13, 2007. This work was supported in part by the College of Science at the Rochester Institute of Technology, the Chester F. Carlson Center for Imaging Science at the Rochester Institute of Technology, and Kodak.

K. G. Baum (email: kgb5056@rit.edu), K. Rafferty, and M. Helguera are with the Chester F. Carlson Center for Imaging Science at the Rochester Institute of Technology, Rochester, NY 14623 USA.

E. Schmidt was with the Rochester Institute of Technology, Rochester, NY 14623 USA, during summer break from Honeoye Falls-Lima High School, Honeoye Falls, NY 14472 USA.

D. H. Feiglin and A. Krol are with the Radiology Department at SUNY Upstate Medical University, Syracuse, NY 13210 USA.

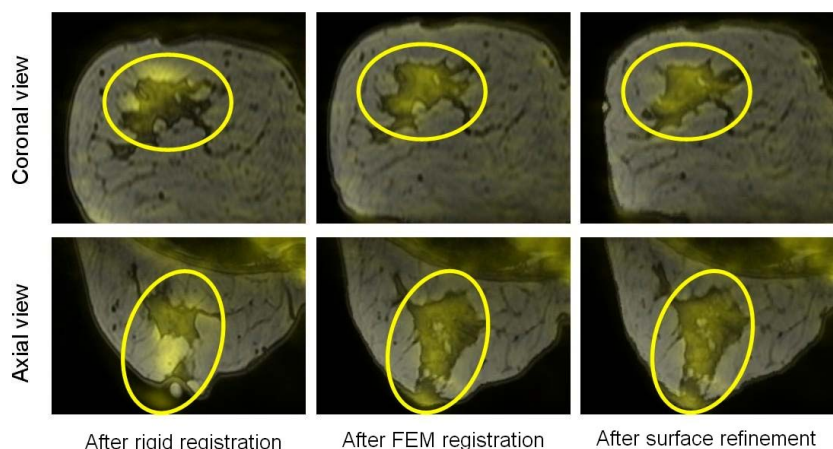


Fig. 1. Registered and fused PET and MRI breast images. Yellow: PET. Gray: MRI. The suspicious lesion area is circled.

here for the nonrigid coregistration of multimodal images overcomes these difficulties because it does not require patient-specific breast morphology and elastic tissue properties.

Identical patient positioning is used to ensure similar stress conditions while obtaining both modalities. Registration occurs as a two step process. During the first step displacement between corresponding fiducial skin markers (FSMs) is used to calculate a displacement field over the entire breast. The specially prepared FSMs are taped to predefined locations on the skin prior to data acquisition, and are visible in all modalities. A dense displacement field is estimated by first distributing the observed FSM displacement vectors linearly over the breast surface and then distributing throughout the volume. This process has been implemented using standard finite element method (FEM) software. Using the resulting displacement field, the MRI image, can be warped to the PET image (Fig. 1).

Since small registration errors still exist in regions away from the FSMs, a surface refinement process is performed. During this phase of registration a large number of corresponding surface points are identified on the warped MRI image and the CT image of the breast that is obtained just before PET (using a PET/CT scanner), and that is coregistered with the PET image. The displacement vectors found between the corresponding points in the MRI and CT images are then used to deform the mesh a second time. The displacement field provided by the mesh is then used to create the registered image (Fig. 1). More information about this registration process can be found in [7, 8]

III. FUSION TECHNIQUES FOR VISUALIZATION

Even when viewing the registered images side by side spatial relationships may be difficult to ascertain. A combined MRI/PET image has the benefits of directly showing the spatial relationships between the two modalities, increasing the sensitivity, specificity, and accuracy of diagnosis.

Several factors need to be considered when choosing a visualization technique. These include information content,

observer interaction, ease of use, and observer understanding. From an information point of view it is desirable to maximize the amount of information present in the fused image. Ideally, the registered images would be viewed as a single image that contains all of the information contained in both the MRI image and the PET image. Limitations in the dynamic range and colors visible on current display devices, as well as limitations in the human visual system make this nearly impossible.

This loss of information can be partially compensated by making the fused display interactive. Some sort of control over the fusion technique can be provided which allows the observer to change the information that is visible in the fused display.

The design of this control is an important part of the fusion process. How simple is it to use the control? How much training is required? Do the display options offered by the control aid the observer or just complicate the observation process? How responsive is the control?

The last and perhaps the most important factor relates to the observer's understanding of the fused volume. For example, radiologists understand what they are looking at when they examine a grayscale MRI image, or PET image, i.e. variations in intensity and texture have a meaning. In the ideal case the knowledge and experience the observer has in examining the individual modalities would be directly applicable to the fused images.

Much research has been devoted to discover new and optimum ways to take two images and display them as a single one. These techniques include color overlay, color mixing, techniques based directly on color spaces, and spatial and temporal interlacing. For a review of these techniques see [9].

An interesting fact is that a two dimensional color lookup table (LUT) can be used to implement all of these fusion techniques with the exception of interlacing. Even when using interactive techniques the fusion procedure being used at a given instance in time can generally be described using two dimensional color tables. This work takes advantage of this fact when presenting the fusion techniques studied to the reader.

A. Techniques Studied

Eight promising fusion for visualization techniques were selected by the authors to be investigated further. Each of these techniques is shown in Fig. 2 and discussed below:

1) Fire/Gray

This technique was created using color overlay. The fire color table from ImageJ [10] was applied to the PET image and a grayscale color table to the MRI image. Color was used for PET and variations in intensity for MRI since MRI is a higher resolution modality, and the human visual system is more sensitive to small changes in intensity than to small changes in

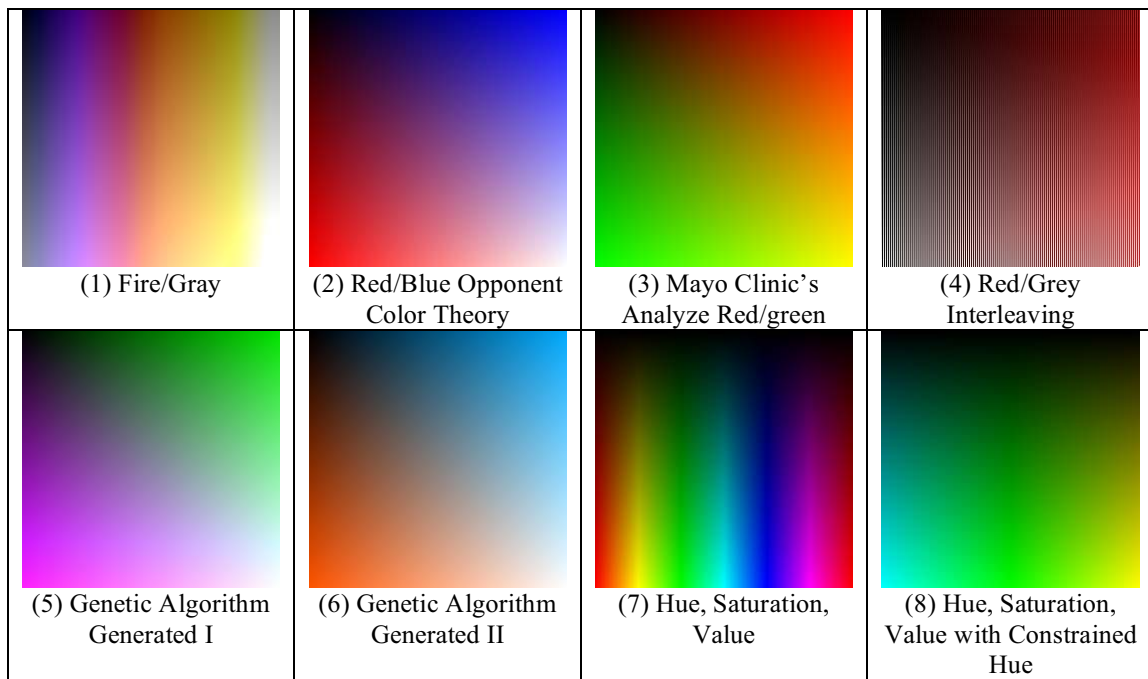


Fig. 2. Color tables for the different fusion techniques investigated in the study. The vertical direction corresponds to the MRI intensity and the horizontal to the PET intensity. The origin is located in the upper left

color [11-13]. The technique was selected for study due to its use in other research.

2) Red/Blue

This technique is based on the CIE $L^*a^*b^*$ color space. It is performed by assigning shades of blue to the PET image and shades of red to the MRI image. These colors are selected based on opponent color theory. The basic assertion of opponent color theory is that red and blue are perceived separately and changes to one, will not affect the perceived amount of the other. This assertion does not necessarily hold for most other color pairs.

3) Red/Green

This is another color overlay technique. A red color table is applied to the PET image and a green color table to the MRI image. It was selected for inclusion in the study because of its use in the Mayo Clinic's Analyze software package [14].

4) Gray/Red Interlace

This fusion technique is based on spatial interlacing. Fused images were created by taking alternating columns from each of the source images. For example, the odd columns in the fused image are taken from odd columns in the PET image while the even columns are taken from even columns in the MRI image. The PET image was first pseudo colored using a red color table. This technique was selected for the study because of its popularity in the research literature [1, 15-16].

5) Genetic Algorithm I

The designed genetic algorithm utilizes the color mixing model to generate color tables that meet specific requirements. In particular it searches for color tables that satisfy the properties proposed by Trumbo [17] along with other simple constraints. These include the order principle, the rows and columns principle, perceivable uniformity and maximized

contrast. More information on the genetic algorithm can be found in [18].

6) Genetic Algorithm II

This technique was also produced using the genetic algorithm previously discussed. A different random initial population, and a different sequence of random mutations, splicing, and selection resulted in a different optimized color table.

7) Hue, Saturation, Value

The hue, saturation, value (HSV) color space is a model designed to describe the humans perceive color. Hue is the color, saturation is the amount of the color, and value is the intensity of the color. A visual representation of this color space is shown in Fig. 3. For this technique hue was used to present the PET image and value was used to present the MRI image. The saturation was kept constant. Like the Fire/Gray technique the MRI was used for the intensity, because of the

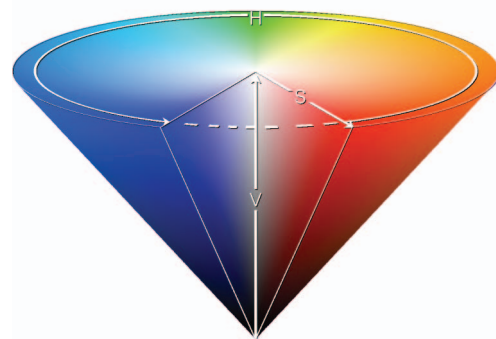


Fig. 3 Conical representation of the HSV color space. Figure from [19], distributed under the Creative Commons Attribution 2.5 Generic license.

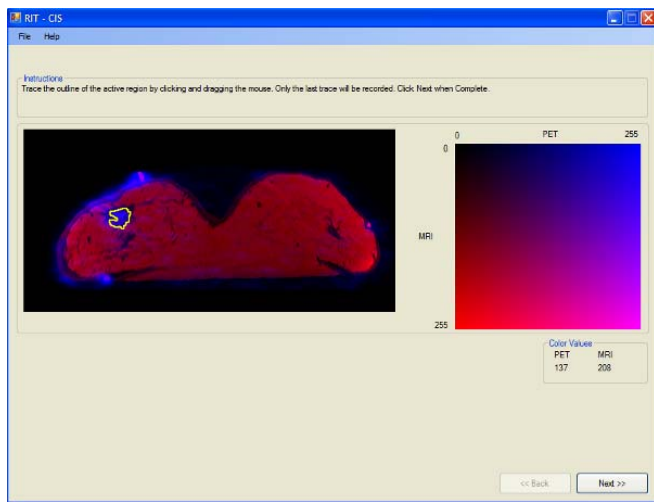


Fig. 4. Interface used by radiologists to evaluate fusion techniques

human visual system's higher sensitivity to changes in intensity over changes in color. This color table was selected because of its popularity throughout the literature.

8) *HSV, Constrained Hue*

This technique is similar to the previously discussed hue, saturation, value technique except that it uses a constrained hue angle. Instead of allowing the color to vary over the entire spectrum, it was only allowed to vary within the cyan to green to yellow region [12]. Constraining the hue angle helps prevent false segmentation due to changes in color, and provides colors that appear to have a natural ordering to a human observer.

B. Fusion Software

Fusion was performed using the Fusion Viewer* software packages. Fusion Viewer is a new application, developed in-house and available for free. It has been designed and implemented in C# with a modular object oriented design for increased extensibility and compatibility, along with simplified distribution.

Fusion Viewer provides both traditional and novel options for displaying and fusing 3D data sets. A simple plug-in interface allows rapid development of novel fusion techniques. In addition to fusion capabilities, several options are provided for mapping 16-bit data sets onto an 8-bit display, including windowing, automatically and dynamically defined tone transfer functions, and histogram based techniques. Also, both traditional maximum intensity projections (MIP) and MIPs of fused volumes are supported. More information on the Fusion Viewer software package can be found at [20-21].

IV. THE STUDY

To test the validity of fusion based visualization techniques the eight techniques previously discussed and shown in Fig. 2 were selected to conduct an exercise with radiologists from the Department of Radiology at SUNY Upstate Medical University. Nine different images with no malignant lesions

were presented in random order using each of the eight techniques and four radiologists were asked to perform the following tasks using the interface shown in Fig. 4.

- (1) On a PET monochrome image click on the region of maximum metabolic activity (glandular tissue).
- (2) On a gray scale LUT select the gray level, on the PET image, that corresponds to the gray level value of the region of maximum activity.
- (3) On an MRI image click on the morphological region that corresponds to the gray level value of the region of maximum metabolic activity (the same location clicked on the PET image).
- (4) On a gray scale LUT select the gray level, on the MRI image, that corresponds to the gray level value of the region of maximum activity.
- (5) Trace the region of maximum metabolic activity on both the PET and MRI images.
- (6) On a fused image click on the region of maximum metabolic activity.
- (7) Click on the corresponding color on the LUT to identify the associated PET and MRI values.
- (8) Trace the region of maximum metabolic activity on the fused image.
- (9) Evaluate degree of difficulty while performing the task.
- (10) Evaluate understanding of the fusion technique used.
- (11) Indicate preference for the fusion technique.

Images used for the study were acquired using a dedicated PET/CT scanner (GE Discovery ST with BGO detector and 4-slice CT) and a 1.5T MRI System (Philips Intera). PET images were obtained with patient prone and breasts freely suspended, immediately after intravenous administration of 10 mCi of F-18-FDG with nine fiducial skin markers (FSMs) taped on the skin of each breast. They were reconstructed in a 128×128×47 matrix, with 4.25 mm voxel size. Each FSM contained 0.5 μ Ci of Ge-68. To assure that the stress conditions in the imaged breast are virtually the same in different modalities, a replica of the MRI breast antenna made of plastic with very low absorption for 511 keV photons in PET scans was used. In MRI scans, the patient was prone with both breasts suspended into a single well housing a standard Philips clinical breast RF receiver coil. A high-resolution 3D Fast Field Echo (FFE) technique with TR/TE = 14/3 was applied to obtain MRI breast images. An image matrix of 512×512×120 was used in reconstruction with 0.7×0.7×1.4 mm³ voxel size. The field of view (360 mm × 360 mm) was centered over the breasts.

The registration was performed using the procedure discussed in Section II. After registration slices through regions of interest were selected from each data set for use in the study. The slices were extracted and fused using the Fusion Viewer application and correspond to the standard views, coronal, sagittal, and axial. The regions of interest were selected to be regions containing above average metabolic activity. Fig. 5 contains examples of images used during the study.

* www.kgbtechnologies.com/fusionviewer/

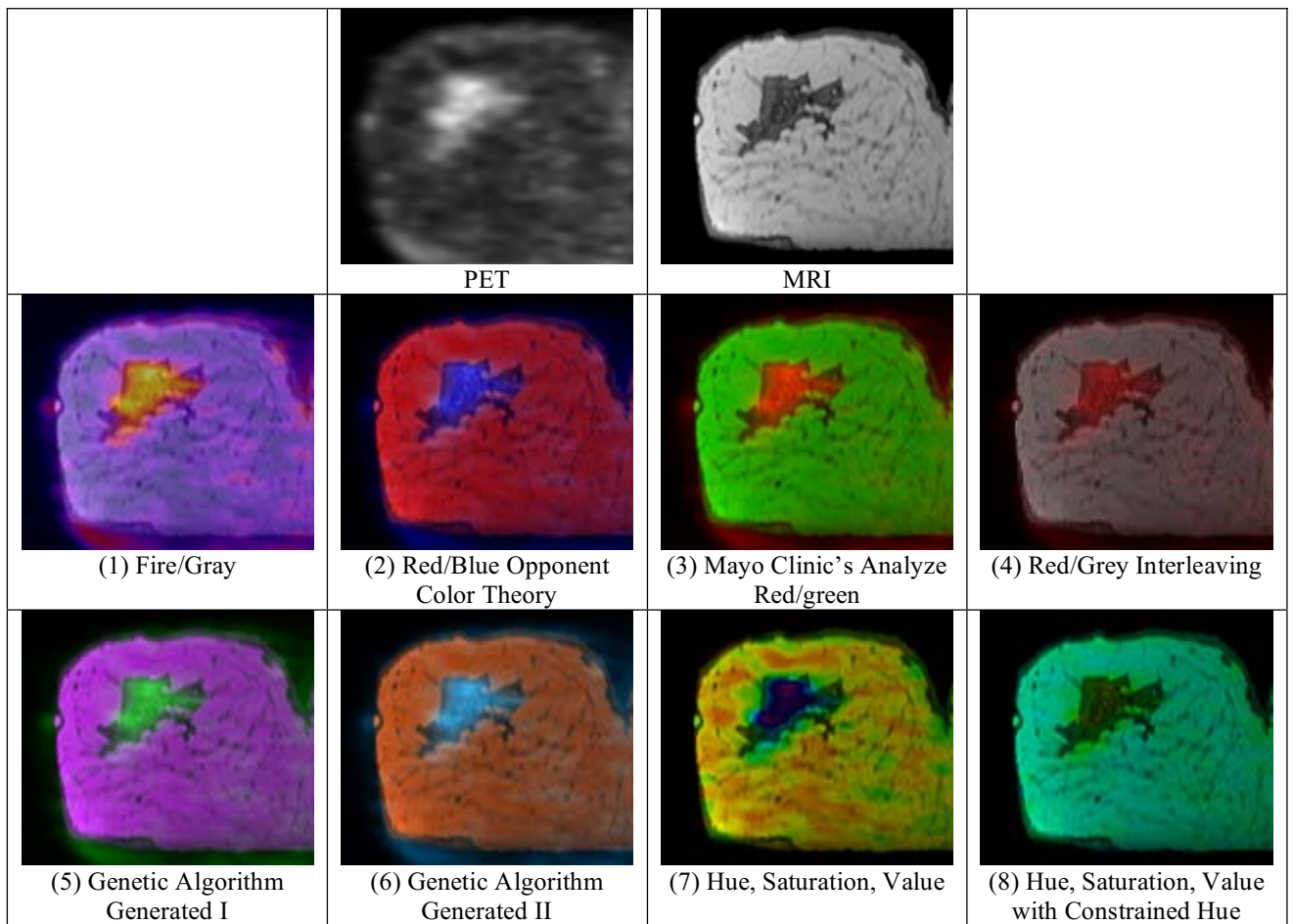


Fig. 5. Fused images created using each technique. The PET and MRI source images used are shown in the top row.

V. RESULTS AND CONCLUSIONS

Figure 6 shows a plot of the mean distance, in pixels, between the location of the area of maximum metabolic activity selected on the MRI and the PET gray scale images when viewed side-by-side. One pixel corresponds to 0.7mm by 0.7mm. All error bars shown here represent the standard error of the mean. It can be seen that the average distance is approximately 10.7 pixels, in other words, there is up to approximately a 1cm difference between the two regions selected when viewing PET and MRI images side by side. This discrepancy increases the risk of performing a biopsy in the wrong location, and justifies the need for a fused display.

Figure 7, on the other hand, shows the mean distance in pixels between the location of the area of maximum metabolic activity selected on the fused image and the corresponding location selected on the gray scale PET image. It can be seen that the average distance is reduced particularly with techniques 5 and 6, which correspond to the two color tables generated by the genetic algorithm. Performance is worst with technique 8, possibly because as the range of colors gets smaller they become increasingly difficult to differentiate.

Figure 8 shows results of the difficulty rating assigned by the observer when performing the tasks with each technique, where 5 represents easiest and 1 represents hardest. It can be

seen that techniques 5 and 6 are ranked the easiest to use. Techniques 1 and 3 also have high rankings, which may reflect past experience using those techniques.

Figure 9 shows the level of understanding that the observer believes they have for each of the techniques. The rankings are fairly even with techniques 3 and 4 having the highest and techniques 7 and 8 the lowest. It is not surprising that 7 and 8 rank the lowest, as it is unlikely that radiologists have significant experience describing colors using HSV color space.

Figure 10 shows the preferences assigned to each technique by the observers. No technique is given significantly higher preference than any other. The higher preferences are assigned to techniques 1, 3, 4, and 6. It is interesting to note that the techniques the observers claimed to prefer and understand the best were not necessarily the ones with which they were best able to complete the tasks. This suggests that thorough testing should be performed before selecting a fusion technique rather than choosing the technique most radiologists seem to prefer.

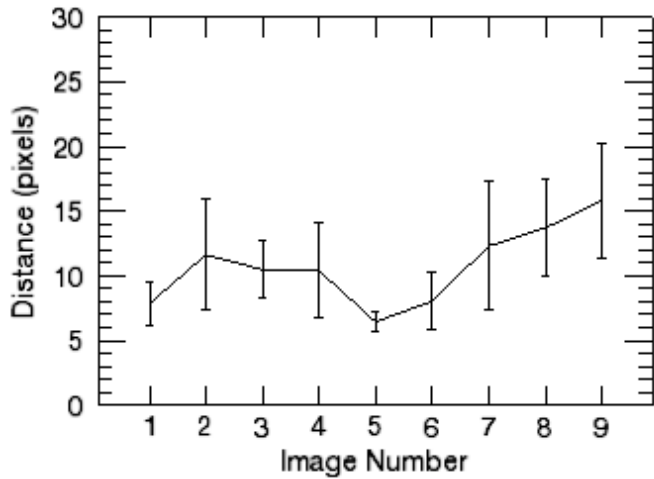


Fig. 6. Mean distance in pixels between corresponding location chosen on PET and MRI image when viewed side-by-side.

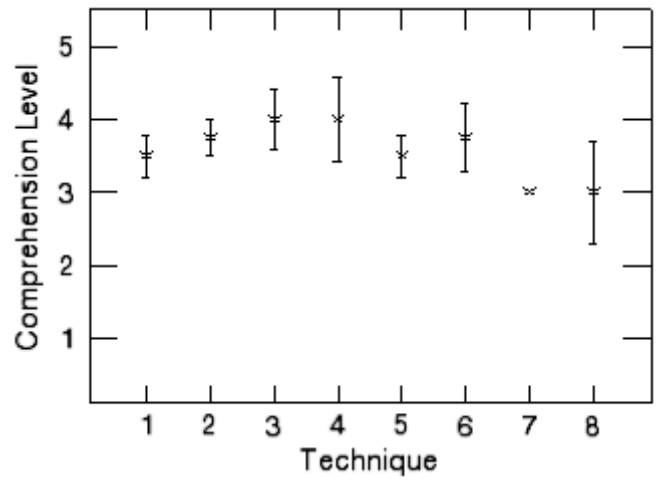


Fig. 9. Comprehension level assigned by observers for each technique. One corresponds to no understanding and five to expert understanding.

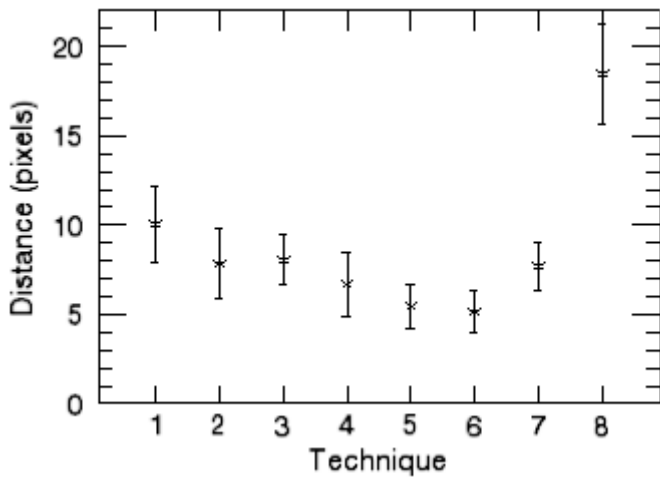


Fig. 7. Mean distance in pixels between corresponding locations chosen on PET and fused image.

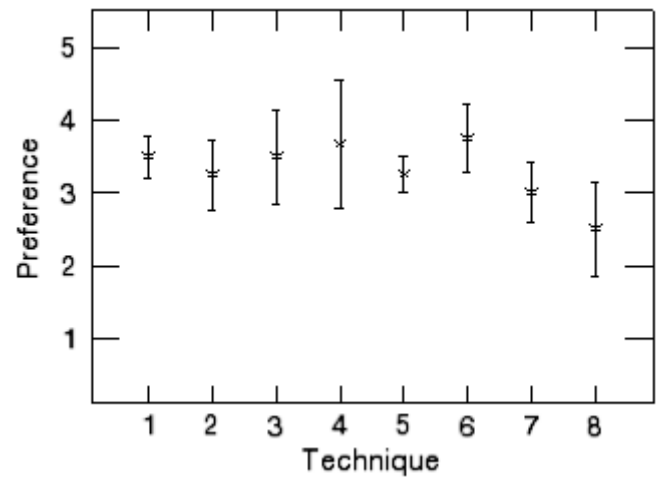


Fig. 10. Preference level assigned by observers for each technique. One corresponds to no preference and five prefer.

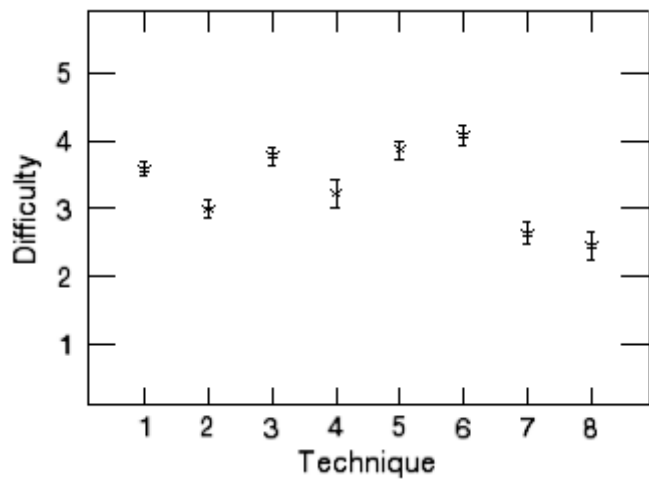


Fig. 8. Difficulty ratings assigned when performing tasks for each technique. One corresponds to hardest and five to easiest.

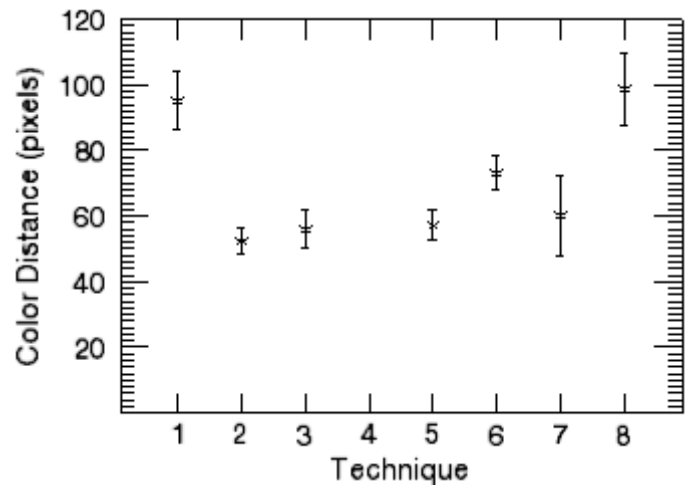


Fig. 11. Mean distance in pixels on the color table between the color observers thought they chose from the fused image and color they actually chose. Maximum distance is 362 pixels.

Figure 11 shows the mean distance on the color tables between the color at a point selected in the fused images and that color as identified on the color table. This distance represents the observer's ability to decode the coloring used for the fusion. It represents the ability of the observer to recover the original MRI and PET value at a given point in the image. Observers achieved the smallest distances with techniques 1, 3, and 5. Technique 4 could not be evaluated with this metric since colors could appear at more than one location in the color table.

The study suggests that the color tables generated by the genetic algorithm, particularly technique 5, are good choices for fusing MRI and PET images. Further details on the study, including the tools used, data used, and data collected can be found in [22]. A larger study evaluating performance of radiologists using the fused images in a clinical setting should be done to further validate the study results. Improvements to the genetic algorithm should be considered, as well as extensions to interactive rather than static fusion techniques.

ACKNOWLEDGMENT

The authors wish to thank Drs. Mary McGrath, Michele Lisi, Mehr Khan, and Daniel Tam, for reading the images.

REFERENCES

- [1] K. Rehm, S. C. Strother, J. R. Anderson, K. A. Schaper, and D. A. Rottenberg, "Display of merged multimodality brain images using interleaved pixels with independent color scales," *J Nucl Med*, vol. 35, pp. 1815-21, 1994.
- [2] E. Bombardieri and F. Crippa, "PET imaging in breast cancer," *Quat. J. Nuc. Med.*, vol. 45, pp. 245-256, 2001.
- [3] K. Scheidhauer, C. Walter, M. D. Seemann, "FDG PET and other imaging modalities in the primary diagnosis of suspicious breast lesions," *Eur. J. Nucl. Med. Mol. Imaging.*, 31, Suppl. 1, S70-S79, 2004.
- [4] P. A., Eliat, and V. Dedieu, et al., "Magnetic resonance imaging contrast-enhanced relaxometry of breast tumors: an MRI multicenter investigation concerning 100 patients," *Mag. Res. Imaging*, vol. 22, pp. 475-81, 2004.
- [5] P. Gibbs, G. P. Liney, et al., "Differentiation of benign and malignant sub-1 cm breast lesions using dynamic contrast enhanced MRI," *Breast* vol. 13, pp. 115-21, 2004.
- [6] A. Samani, J. Bishop, D. B. Plewes, "A Constrained Modulus Reconstruction Technique for Breast Cancer Assessment," *IEEE Trans. Med. Imaging* 20(9), 877-885, 2001.
- [7] I. Coman, A. Krol, D. Feiglin, E. Lipson, J. Mandel, K. G. Baum, M. Unlu, and L. Wei, "Intermodality nonrigid breast-image registration," *Proc. IEEE International Symposium on Biomedical Imaging*, vol. 2, pp. 1516-1519, 2004.
- [8] A. Krol, M.Z. Unlu, K. G. Baum, J. A. Mandel, W. Lee, I. L. Coman, E. D. Lipson, D. H. Feiglin; "MRI/PET Nonrigid Breast-Image Registration Using Skin Fiducial Markers," *Physica Medica European Journal of Medical Physics*, vol. 21, Suppl. 1, pp. 39-43, 2006.
- [9] K. G. Baum, M. Helguera, J. P. Hornak, J. P. Kerekes, E. D. Montag, M. Z. Unlu, D. H. Feiglin, A. Krol, "Techniques for Fusion of Multimodal Images: Application to Breast Imaging," *Proceedings International Conference on Image Processing*, pp. 2521-2524, 2006.
- [10] NIH, "ImageJ, Image Processing and Analysis in Java," available at <http://rsb.info.nih.gov/ij/>, accessed Nov. 5, 2007.
- [11] J. C. Russ, *The Image Processing Handbook*, Fourth ed: CRC Press, Inc., 2002.
- [12] A. T. Agoston, B. L. Daniel, R. J. Herfkens, D. M. Ikeda, R. L. Birdwell, S. G. Heiss, A. M. Sawyer-Glover, "Intensity-modulated parametric mapping for simultaneous display of rapid dynamic and high-spatial-resolution breast MR imaging data," *Radiographics*, vol. 21, pp. 217-26, 2001.
- [13] M. K. Sammi, C. A. Felder, J. S. Fowler, J.-H. Lee, A. V. Levy, X. Li, J. Logan, I. Palyka, W. D. Rooney, N. D. Volkow, G.-J. Wang, C. S. Springer Jr, "Intimate Combination of Low- and High-Resolution Image Data: I. Real-Space PET and H₂O MRI, PETAMRI," *Magnetic resonance in medicine*, vol. 42, pp. 345-360, 1999.
- [14] Mayo Clinic's Biomedical Imaging Resource, "Analyze Software System," available at <http://www.mayo.edu/bir/Software/Analyze/Analyze1NEW.html>, accessed Nov. 5, 2007.
- [15] P. G. Spetsieris, V. Dhawan, T. Ishikawa, D. Eidelberg, "Interactive visualization of coregistered tomographic images," *Biomedical Visualization Conference*, Atlanta, GA, USA, 1995.
- [16] J. S. Lee, B. Kim, Y. Chee, C. Kwark, M. C. Lee, K. S. Park, "Fusion of coregistered cross-modality images using a temporally alternating display method," *Med. Biol. Eng. Comput.*, vol. 38, pp. 127-32, 2000.
- [17] B. E. Trumbo, "Theory for Coloring Bivariate Statistical Maps," *The American Statistician*, vol. 35, no. 4, pp. 220-226, 1981.
- [18] K. G. Baum, M. Helguera, A. Krol, "Genetic Algorithm Automated Generation of Multivariate Color Tables for Visualization of Multimodal Medical Data Sets," *Proc. IS&T/SID fourteenth Color Imaging Conference*, pp. 138-143, 2006.
- [19] Wikipedia, "HSL Color Space," available at http://en.wikipedia.org/wiki/HSV_color_space, accessed Nov. 5, 2007.
- [20] K. G. Baum, M. Helguera, A. Krol, "A New Application For Displaying and Fusing Multimodal Data Sets," *Proc. of SPIE Multimodal Biomedical Imaging II*, vol. 6431, pp. 64310Y, 2007.
- [21] K. G. Baum, M. Helguera, A. Krol, "Fusion Viewer: A New Tool for Fusion and Visualization of Multimodal Medical Data Sets," *Journal of Digital Imaging*, in press, available online through SpringerLink Online First.
- [22] K. Rafferty, K. G. Baum, E. Schmidt, A. Krol, M. Helguera, "Multimodal Display Techniques with Application to Breast Imaging," *RIT Digital Media Library*, available at <http://hdl.handle.net/1850/4648>, 2007.